ACCOUNTS
of chemical research

Strategies for the Synthesis of Supported Gold Palladium Nanoparticles with Controlled Morphology and Composition

GRAHAM J. HUTCHINGS*,† AND CHRISTOPHER J. KIELY‡

†Cardiff Catalysis Institute, School of Chemistry, Cardiff University, Main Building, Park Place, Cardiff CF10 3AT, United Kingdom, and ‡Department of Materials Science and Engineering, Lehigh University, 5 East Packer Avenue, Bethlehem, Pennsylvania,18015, United States

RECEIVED ON JANUARY 4, 2013

CONSPECTUS

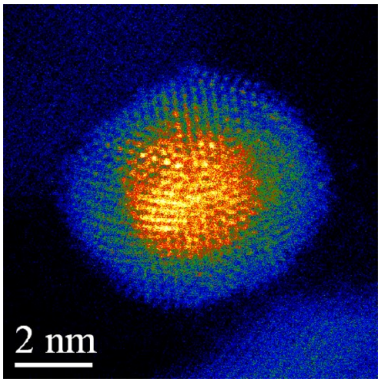

The discovery that supported gold nanoparticles are exceptionally effective catalysts for redox reactions has led to an explosion of interest in gold nanoparticles. In addition, incorporating a second metal as an alloy with gold can enhance the catalyst performance even more. The addition of small amounts of gold to palladium, in particular, and vice versa significantly enhances the activity of supported gold–palladium nanoparticles as redox catalysts through what researchers believe is an electronic effect.

In this Account, we describe and discuss methodologies for the synthesis of supported gold–palladium nanoparticles and their use as heterogeneous catalysts. In general, three key challenges need to be addressed in the synthesis of bimetallic nanoparticles: (i) control of the particle morphology, (ii) control of the particle size distribution, and (iii) control of the nanoparticle composition. We describe three methodologies to address these challenges. First, we discuss the relatively simple method of coimpregnation. Impregnation allows control of particle morphology during alloy formation but does not control the particle compositions or the particle size distribution. Even so, we contend that this method is the best preparation method in the catalyst discovery phase of any project, since it permits the investigation of many different catalyst structures in one experiment, which may aid the identification of new catalysts. A second approach, sol-immobilization, allows enhanced control of the particle size distribution and the particle morphology, but control of the composition of individual nanoparticles is not possible. Finally, a modified impregnation method can allow the control of all three of these crucial parameters. We discuss the effect of the different methodologies on three redox reactions: benzyl alcohol oxidation, toluene oxidation, and the direct synthesis of hydrogen peroxide. We show that the coimpregnation method provides the best reaction selectivity for benzyl alcohol oxidation and the direct synthesis of hydrogen peroxide. However, because of the reaction mechanism, the sol-immobilzation method gives very active and selective catalysts for toluene oxidation. We discuss the possible nature of the preferred active structures of the supported nanoparticles for these reactions. This paper is based on the *IACS Heinz Heinemann Award Lecture* entitled "*Catalysis using gold nanoparticles*" which was given in Munich in July 2012.

Introduction

Supported metal nanoparticles containing gold are of immense importance in the field of heterogeneous catalysis.[1,2] Gold by virtue of its nobility was considered to be of no interest as a catalyst since it would not be expected to engender reactivity. Yet in the periodic table it is surrounded by elements that are used in a number of commercial catalysts (Figure 1). It is therefore surprising that catalysis using gold was not investigated sooner that it was. However, since two seminal studies in the 1980s,[3−6] it is now known that gold, when dispersed as nanoparticles comprising a few tens or hundreds of atoms, is an exceptionally effective redox catalyst leading to an explosion of interest in gold catalysis.[2,7−16] There is a general consensus that small gold nanoparticles are important,[2,7−10,12−16] and recent studies show that small gold nanoclusters/bilayers are important.[17] Hence, there is a need to identify strategies that can prepare small nanoparticles. However, this can be

Published on the Web 04/15/2013 www.pubs.acs.org/accounts
10.1021/ar300356m

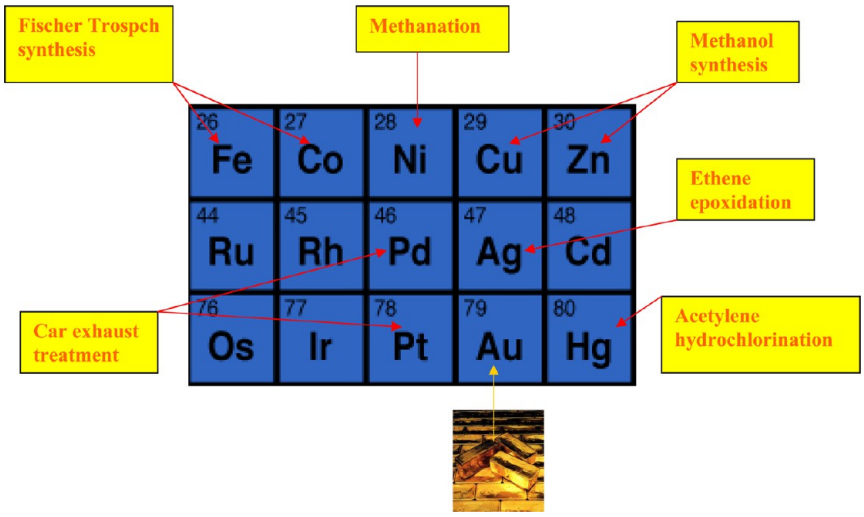

FIGURE 1. Periodic table with elements around Au used in in commercial catalysts.

problematic; for example, supporting Au_{55} on carbon gave a broad particle size distribution.[18] We therefore need effective strategies for the synthesis of nanoparticles with controlled particle size distributions.

Alloying a second metal with gold has been found to enhance the activity significantly. This is considered to act by an electronic effect and the addition of palladium to gold leads to catalysts that are active for the direct synthesis of hydrogen peroxide[19] (Scheme 1), the oxidation of alcohols[20] (Scheme 2), and the oxidation of hydrocarbons[21] (Scheme 3). The enhancement in activity can also be observed with gold–platinum catalysts,[22] but characterization of these catalysts is more facile using scanning transmission electron microscopy for the gold–palladium catalysts due to the mass (*z*-) contrast between the two elements. Introducing a second metal, however, leads to a new synthetic problem, namely, that the concentrations of the two metals can vary between nanoparticles and in particular with the size of the nanoparticles. Hence, in the synthesis of supported bimetallic nanoparticles, there are two potential problems that have to be overcome, that is, controlling both size and composition distributions of the materials.

In this Account, we discuss three relatively simple methods by which supported gold–palladium nanoparticles can be fabricated, namely coimpregnation (C_{Im}), sol-immobilization (S_{Im}), and modified-impregnation (M_{Im}). We show the key features of the materials that are made, from both a morphological and composition distribution viewpoint, but also from the standpoint of their catalytic efficacy. We aim to show that preparation methodologies now exist that permit the control of both the particle size distribution and the composition of the individual nanoparticles. This is an important advance for optimizing the catalytic performance of these supported nanoparticles.

SCHEME 1. Selective Formation of H_2O_2 (k_1) and the Nonselective Processes of Hydrogenation (k_2), Combustion (k_3), and Decomposition (k_4)

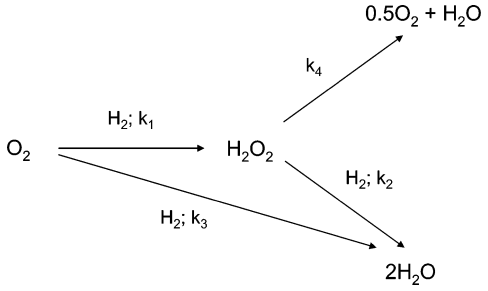

Throughout this Account, we present a wide range of analytical electron microscopy data. Particle size distributions were assessed using a combination of (i) phase contrast transmission electron microscopy (TEM) (1–20 nm), (ii) backscattered electron scanning electron microscopy (SEM) imaging (20–1000 nm), and (iii) aberration corrected high angle annular dark field (HAADF) STEM imaging (<1 nm). Atomic mass (*z*-) contrast inherent to HAADF imaging was also used extensively to study the elemental segregation of the Pd and Au components in particles designed to have specific core–shell morphologies, and quantitative compositional analyses of individual alloy nanoparticles were done using the X-ray energy dispersive spectroscopy (XEDS) technique in an aberration corrected STEM.

Preparation of Supported AuPd Nanoparticles Using Coimpregnation

Coimpregnation of metal salts onto a support followed by heat treatment represents one of the most facile ways to

SCHEME 2. Oxidation of Benzyl Alcohol (1) to Benzaldehyde (2) and Nonselective Byproducts: Benzoic Acid (3), Toluene (4), Benzene (5), and Benzylbenzoate (6)

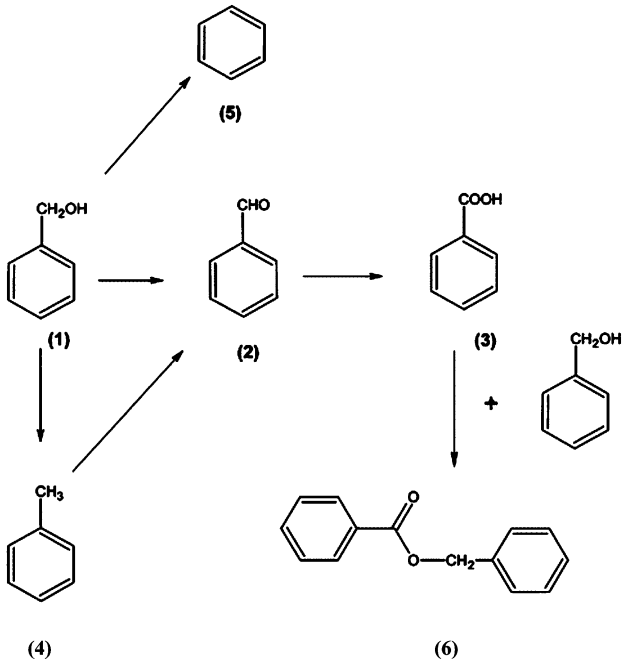

SCHEME 3. Oxidation of Toluene (1) Leading to Benzyl Alcohol (2), Benzaldehyde (3), Benzoic Acid (4), Hemiacetyl (5), and Benzylbenzoate (6)

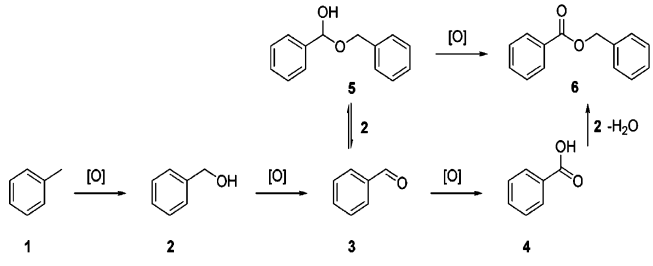

prepare supported metal nanoparticles catalysts.[19,20] In this method, $HAuCl_4$ is dissolved in water and then $PdCl_2$ is dissolved in the resulting acidic solution. The amounts of the metal salts are tailored to the desired nominal ratio of the metal required, and the concentration of the impregnation solution is governed by the porosity of the selected support. The support is then contacted with the solution so that the resulting mixture has the consistency of a smooth paste, as too much water can be detrimental.[23] The paste is then dried (110 °C, 16 h) and calcined (400 °C, 3 h). Both of these heat treatment stages are very important and control the final morphology obtained. The material prepared presents a bimodal distribution of nanoparticles (Figure 2A),[24] all being alloys of Au and Pd (Figure 2B). However, there is a size-dependent effect on the composition of the nanoparticles.[24] The small nanoparticles comprise mainly Pd, and the larger nanoparticles comprise mainly Au (Figure 3).[25] Hence, although this is a very simple method of preparation, it leads to the synthesis of a complex range of nanostructures. In addition, with this method of preparation, there is another level of complexity; namely, that on carbon supports random AuPd alloys are formed following the calcination step, whereas for oxide-supported materials core-shell structures are formed with a gold-rich core and a palladium-rich shell (Figure 4).[20] This forms during calcination as shown in Figure 5.[25]

With this wide range of supported nanostructures, one might be tempted to conclude that the materials made by impregnation would be ineffective as catalysts, but this is far from the case. Indeed, our hypothesis is that this method is ideal for the catalyst discovery phase of any investigation since with such a wide variation in nanostructures available some of them will exhibit activity, and then in subsequent stages of the study the required nanostructures can be identified and synthesized using more appropriate methodologies.

$AuPd/TiO_2$ prepared by coimpregnation is an exceptionally active catalyst for the oxidation of alcohols under solvent-free mild reaction conditions leading to very high yields of the desired aldehyde product in relatively short reaction times (Figure 6).[20] In addition, the same catalyst is very active and selective for the direct synthesis of hydrogen peroxide from its elements.[21] As noted earlier, calcination is very important in forming the core–shell structures on oxide supports (Figure 5) but this also decreases the catalyst activity. However materials calcined at 400 °C the core–shell structures are fully developed and these catalysts are fully stable for many reuses in this reaction.[26] Furthermore, the carbon-supported catalyst is significantly more active and selective for the direct synthesis of H_2O_2. When the carbon support is pretreated with dilute nitric or acetic acid prior to the deposition of the metals, then the resulting catalyst displays very high activity in the direct synthesis reaction at 2 °C[26] and the selectivity based on H_2 consumption is >98%. When this catalyst is stirred with dilute H_2O_2 aqueous solutions in the presence of high pressure H_2 at 2 °C, no decomposition/hydrogenation is observed for 30 min even at concentrations up to 16 vol %.[26] The calcination stage of the catalyst preparation is crucial to fully oxidize the surface Pd as Pd^0 is considered to catalyze H_2O_2 hydrogenation/decomposition.[27]

Hence, the catalysts prepared using the coimpregnation method produce highly selective catalysts for these redox reactions and also display appreciable activity. However, it is logical that only a small proportion of the nanostructures

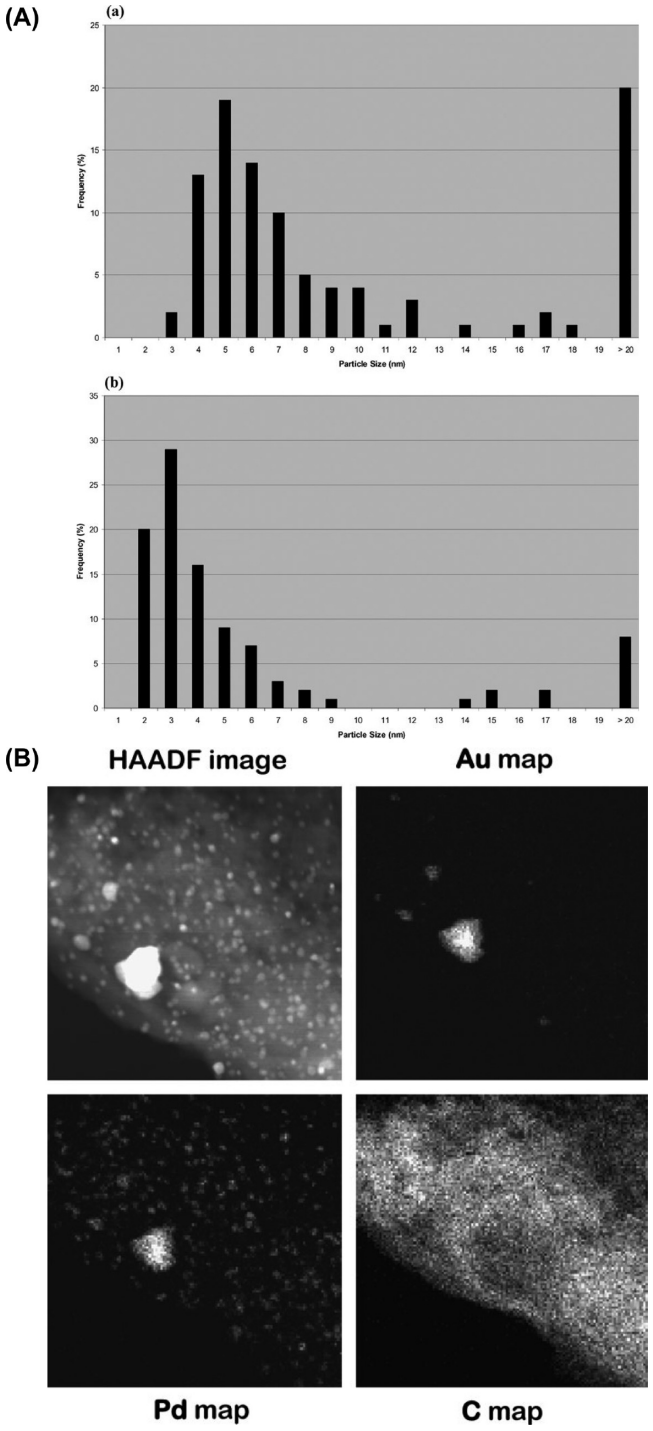

FIGURE 2. (A) Particle size distributions for Au−Pd C_{lm} catalysts (a) Au−Pd/carbon and (b) Au−Pd/TiO_2. (B) HAADF STEM image and Au, Pd, and C STEM XEDS maps for the uncalcined 2.5 wt % Au−2.5 wt % Pd/carbon sample.

that are present are active in the catalysis. We hypothesized that is was the small nanoparticles that could well be the active species, and therefore, we set out to tailor make these structures. We decided to use a sol-immobilization method as previously Rossi and co-workers had shown that this method could produce highly active gold monometallic supported catalysts for alcohol oxidation.[28]

Preparation of Supported AuPd Nanoparticles Using Sol-Immobilization

The intention of using sol-immobilization is that one can make tailor-made morphologies with the desired narrow particle size ranges. The method is relatively noncomplex, and the methods we use involve dissolving $HAuCl_4$ and $PdCl_2$ in a dilute solution of polyvinyl alcohol (PVA). The role of the PVA is to coat the nanoparticles so that they resist sintering during subsequent synthesis steps. A reducing agent is then added, in our case sodium borohydride, and this forms a sol of homogeneous AuPd nanoparticles which can then be readily supported onto carbon or TiO_2 (or other supports).[29,30] There are many stabilizing ligands and reducing agents that can be used. This method can be modified to produce core−shell structures by initially forming either the Au or Pd nanoparticles first and then using these as templates for the deposition of the second metal (Figures 7−9). The as prepared Au + Pd sol (Figure 7a and b) consisted of a mixture of icosahedral (Ih), decahedral (Dh), and cuboctahedral (co) particles, with sizes in the 1−5 nm range. All of the particles greater than ca. 1.5 nm in size showed speckle type intensity variations indicative of random alloying between Au and Pd. For example, a 2 nm cuboctahedral Au + Pd mixed alloy particle is highlighted in Figure 7a (inset), where the brighter columns are Au-rich due to the *Z*-contrast between Au and Pd. Several nanometer scale clusters of atoms are also present in the colloidal sols (indicated by circles). These are possibly homogeneously nucleated structures that form at a later stage during the reduction of metal salts. STEM-HAADF images of the Au shell−Pd core colloids supported on a continuous carbon film are shown in Figure 7c−e. Particles with several distinctive morphologies were noted, including Ih, Dh, co, dodecahedral (DDh), and singly twinned particles (STP). There is a characteristic *Z*-contrast effect noticeable in Figure 7c, where the center of the particle has a considerably lower intensity than the periphery, suggesting a $Pd_{core}-Au_{shell}$ nanostructure or a hollow center in the nanostructure. The $Pd_{core}-Au_{shell}$ interpretation of the contrast shown in a detailed STEM-XEDS spectrum image analysis of such a particle is presented in Figure 8. An entire XEDS spectrum was acquired at each pixel point of ADF image shown in Figure 8a. The summed XEDS spectrum from the entire particle is shown in Figure 8b and confirms that both Au and Pd are present. The spatial distributions of Au and Pd as extracted from the spectrum image datacube are shown in Figure 8c and d, respectively, and a composite RGB image color

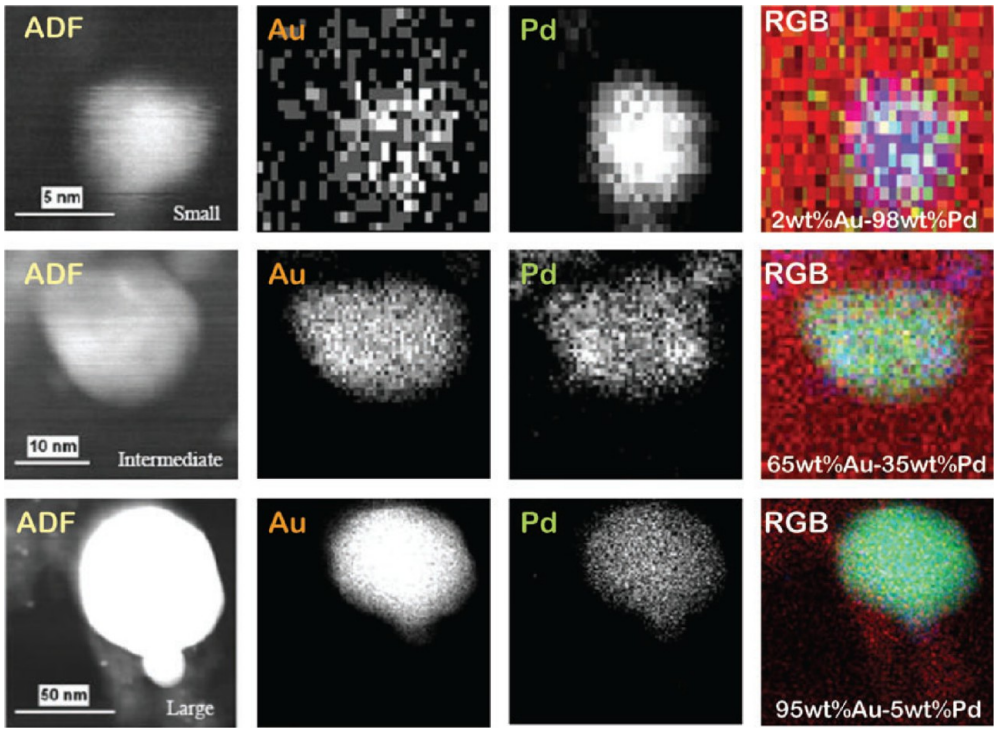

FIGURE 3. Montage of AuPd/C catalyst particles of different sizes: ADF image, Au L_α XEDS map, Pd L_α XEDS map, and RGB overlays (red, C; green, Au; blue, Pd).

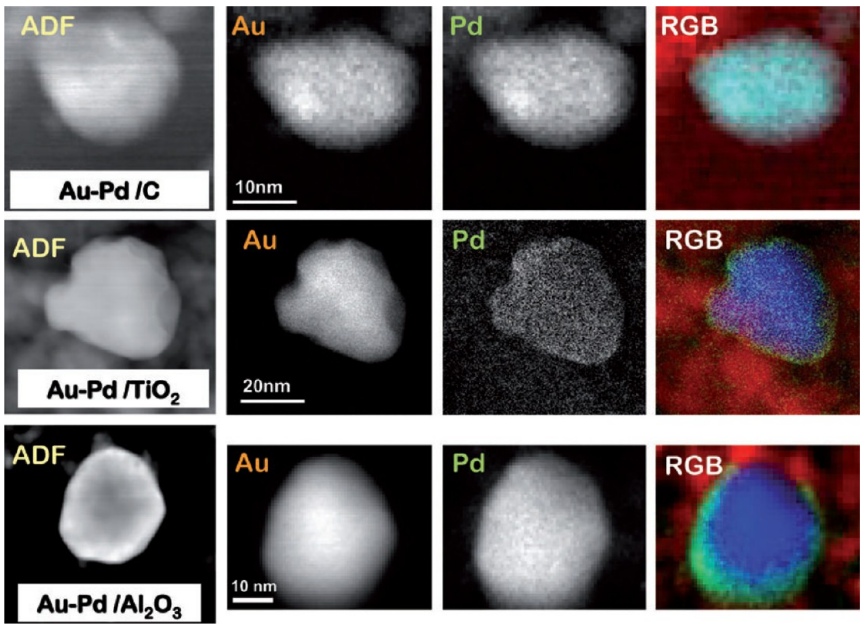

FIGURE 4. Montage of HAADF image: Au, Pd and RGB reconstructed overlay RGB map (Au, blue; Pd, green) for calcined catalysts on three different supports.

overlay map is presented in Figure 8e. Summed spectra extracted from the center and periphery regions of the nanoparticle are shown in Figure 8f and g. It is evident from the STEM-XEDS map that the particle has a core–shell structure with a Pd-rich core and a Au-rich shell. The key aspect is that the neither the core nor the shell region is exclusively one metal, and hence they represent alloys with a concentration gradient across the nanostructure.

It is apparent that the morphology of the sols is not lost when they are supported and dried in this way (Figure 9).

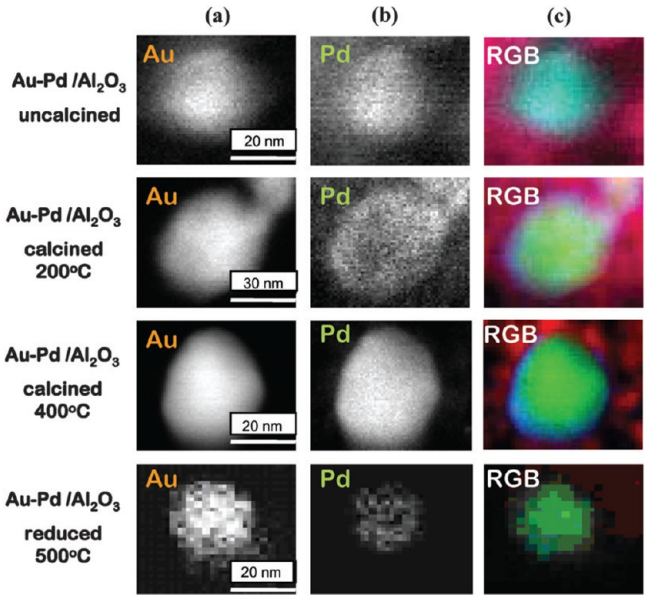

FIGURE 5. Au, Pd XEDS maps and RGB overlays (green, Au; blue, Pd) for a series of $AuPd/Al_2O_3$ catalysts. On calcination, the core–shell structure develops.

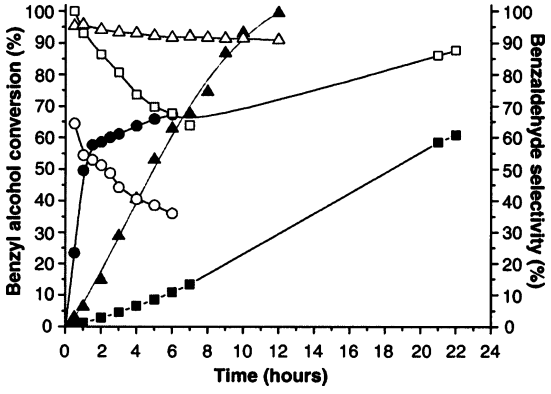

FIGURE 6. Benzyl alcohol reaction at 100 °C, 0.2 MPa O_2 pressure: (■) Au/TiO_2, (●) Pd/TiO_2, and (▲) $Au–Pd/TiO_2$. Solid symbols, conversion; open symbols, selectivity. Reaction carried out in a stirred autoclave with benzyl alcohol (40 mL) and catalyst (20 mg) in the absence of solvent.

Overall, the method typically produces sols with mean particle sizes in the range of 3 nm and supporting the sols does not increase the mean particle size significantly.[29] So this represents a facile way of preparing nanoparticles with a narrow particle size and controlled morphology. However, the carbon- and TiO_2-supported nanoparticles do exhibit a key difference. On carbon, the nanoparticles do not appear to wet the support and the particles are very prone to sintering when they are heated above 200 °C. On TiO_2, the nanoparticles interact with the support and this becomes very marked when they are heat treated (Figure 10), and the nanoparticles are very resistant to sintering. However, both materials show a systematic variation for random alloy

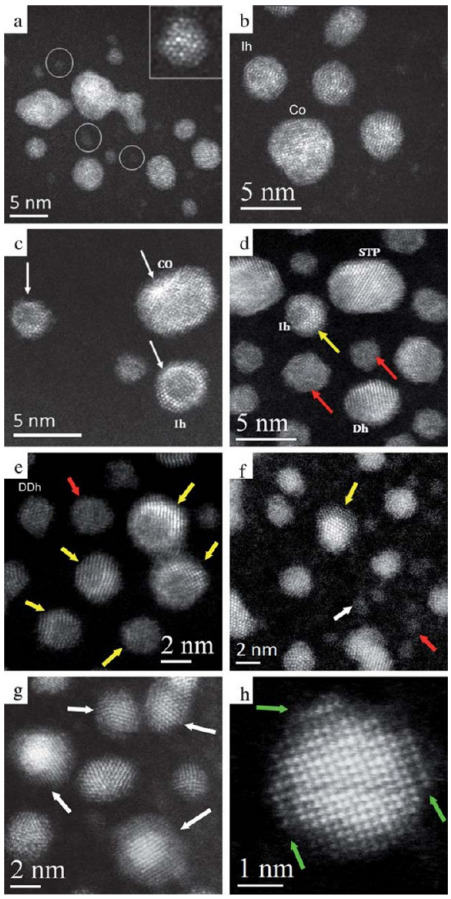

FIGURE 7. STEM HAADF images: (a, b) homogeneous Au + Pd colloids; (c–e) Au shell and Pd core colloids; and (f–h) Pd shell and Au core colloids.

nanoparticles in the composition of the nanoparticles with particle size (Figure 11).[30] However, now the small nanoparticles comprise mainly Au and the larger nanoparticles comprise mainly Pd; that is, this is totally the opposite trend to that observed for the coimpregnation catalysts as described earlier. Hence, although this method can lead to control of the particle size distribution and the particle morphology, it does not overcome the problem of particle size/composition variation.

Of course the key question is this: are these smaller nanostructures active and selective as catalysts? Indeed, they are very active, being 10 times more active than coimpregnated catalysts, with this difference in activity being due to the smaller nanoparticle sizes that can be prepared.[30] However, they are much less selective and they produce much lower yields of benzaldehyde and higher amounts of benzoic acid and benzylbenzoate (Scheme 2). The method does allow for the preparation of a range of nominal compositions very easily.[30] It is found that the addition of a small amount of Au to Pd, and vice versa, significantly enhances the catalyst activity for both benzyl alcohol oxidation and the direct synthesis of hydrogen peroxide (Figure 12a). The activities observed

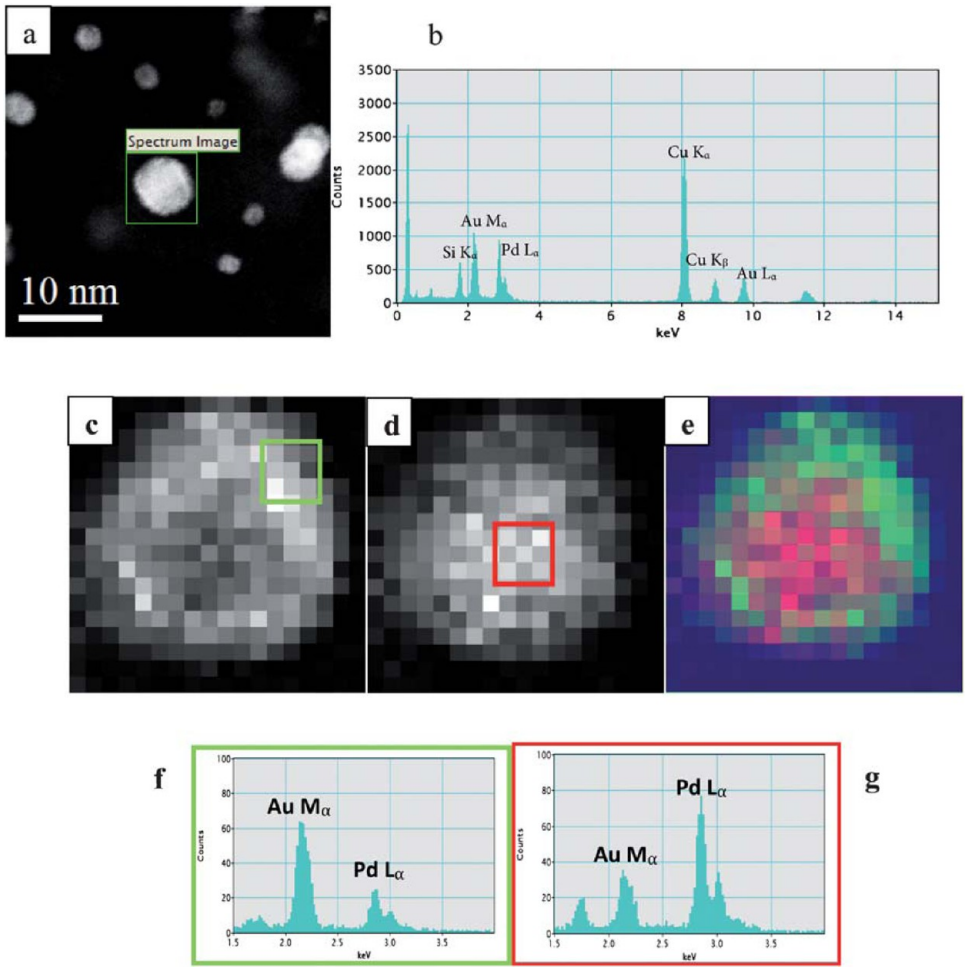

FIGURE 8. (a) ADF image selected for STEM-XEDS mapping; (b) XEDS; (c, d) Au, Pd elemental maps of the nanoparticle obtained after MSA processing; (e) distribution of Au (green) and Pd (red; (f, g) cumulative XEDS spectra from 3 × 3 pixels (indicated by squares in (c and d)) from the center and periphery of the particle, respectively.

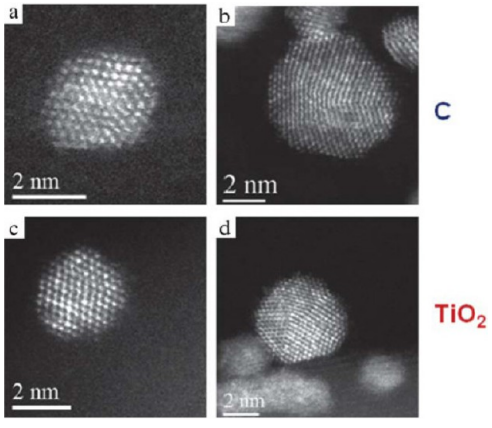

FIGURE 9. STEM-HAADF images of individual Au + Pd S_{Im} nanoparticles on (a, b) activated C and (c, d) TiO_2 supports, after drying at 120 °C for 16 h.

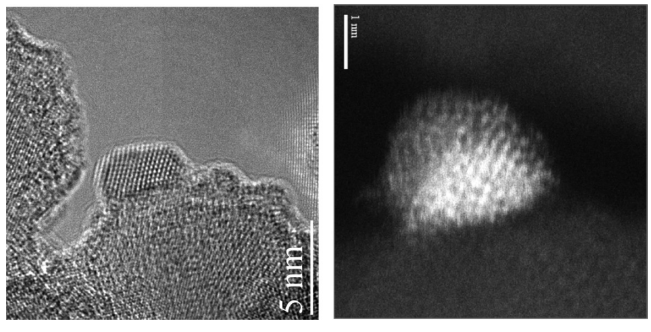

FIGURE 10. HREM micrograph and STEM-HAADF image TiO_2-supported Au shell−core Pd S_{Im} nanoparticles after calcination at 400 °C for 3 h.

for the homogeneous alloys are exceptionally high, but unfortunately the selectivities are low. This is illustrated for the direct synthesis of hydrogen peroxide since the rate of hydrogen peroxide hydrogenation/decomposition is roughly three times that of the synthesis reaction (Figure 12b). It is therefore clear that, for both of these reactions, the small nanoparticle structures, facilitated by the sol-immobilization method, are not the highly selective species that are present in the materials prepared by coimpregnation that demonstrate

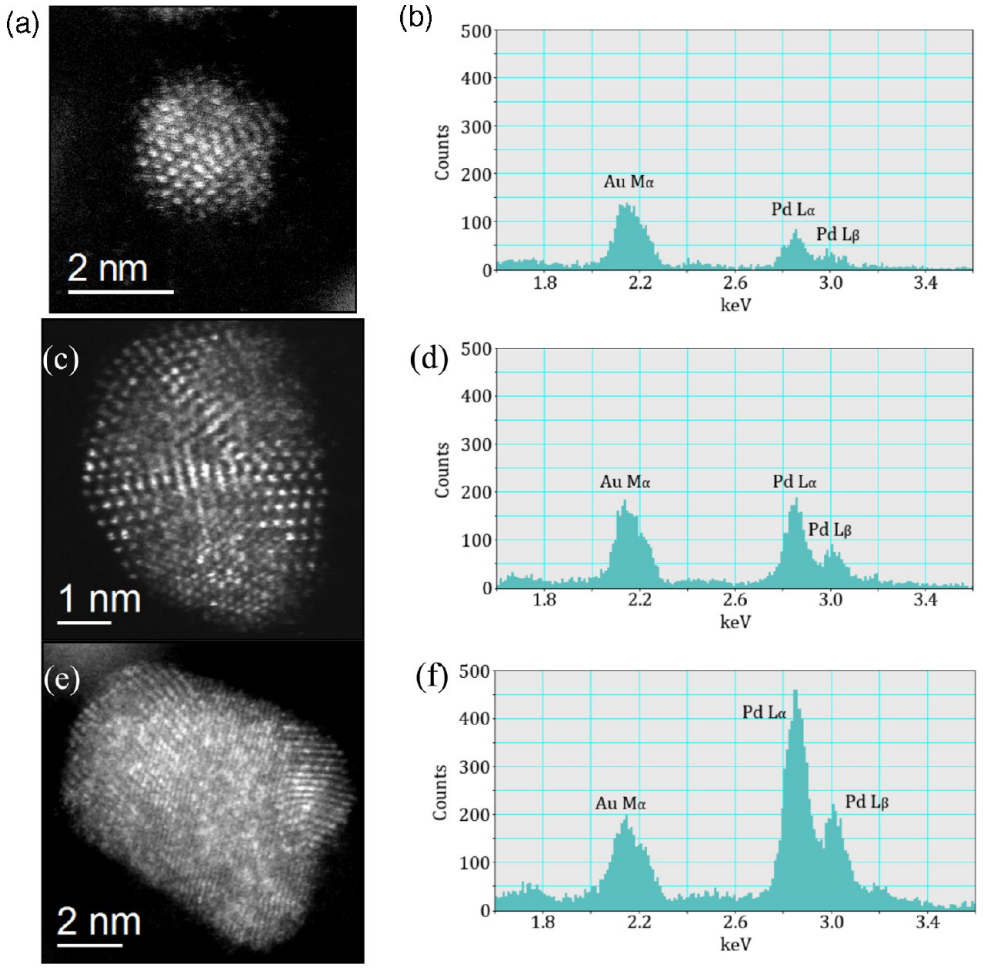

FIGURE 11. HAADF images and corresponding XEDS point spectra of Au + Pd nanoparticles of progressively increasing size with a nominal composition of Au/Pd = 1:7.

exceptionally high selectivities. Hence, it is apparent that our hypothesis that the smallest nanostructures are the desired materials for effective catalysis has not been substantiated, and it is most likely that larger nanostructures need to be investigated. It is unfortunate that such elegant nanostructures display much lower selectivity. As the catalysts were very active, we investigated them for the oxidation of a significantly less reactive substrate, namely, the activation of the primary C−H bonds in toluene.[21] In this case, the oxidation is very selective for the formation of benzoyl benzoate (Figure 13), and by fine-tuning the reaction conditions, yields of benzoyl benzoate of 96% can be achieved.[21] The high specificity to this single product is due to the reaction scheme as the oxidation proceeds via the initial formation of benzyl alcohol which is rapidly oxidized to benzaldehyde (Figure 6). Benzyl alcohol and benzaldehyde then react to form a hemiacetyl that is oxidized to the ester. In this way, benzoic acid, which could be expected to be the major product is not formed in significant amounts.[21] Hence, the supported nanoparticles prepared using the sol-immobilization method can find efficacy for oxidation reactions. In particular, we showed that these sol-immobilized catalysts can be recovered and reused several times without loss of catalytic performance and also with retention of the nanoparticle morphology.

There is a major problem with S_{Im} catalysts, namely, that once the immobilized nanoparticles are formed they remain coated with the stabilizing ligand, in our case PVA. Although this does not appear to cause significant problems in catalysis with liquid reactants, it does cause major problems if the catalysts need to be used for the reaction of gases, for example, carbon monoxide oxidation. One way of removing the stabilizing ligand is to heat treat the materials in air, but this invariably leads to the loss of the small nanoparticles through sintering.[31] We addressed this problem as we reasoned that once the sol-nanoparticle was supported, the stabilizing ligand can be removed by treatment with a suitable solvent. PVA being water-soluble can be removed by treatment with water at 90 °C, enabling the catalysts to be used for gas phase reactants.[32]

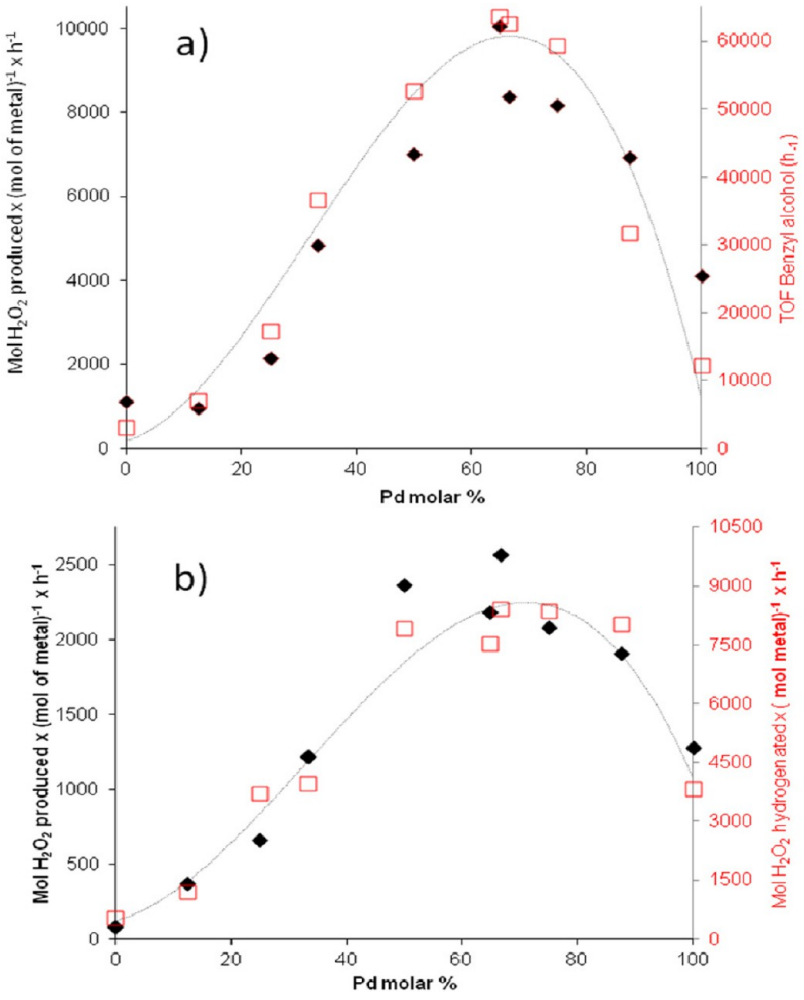

FIGURE 12. S_{Im} Au−Pd/C (a) (◆) H_2O_2 productivity calculated after 2 min reaction (left axis) and (□) TOF of benzyl alcohol calculated after 30 min reaction (right axis). (b) (◆) H_2O_2 productivity calculated after 30 min (left axis) and (□) rate of H_2O_2 hydrogenation calculated after 30 min.

There remains one problem that is apparent for both the coimpregnation method and the sol-immobilized method, namely, the variation in the composition of the nanoparticle with increasing particle size. We have addressed this using a modified impregnation method. We chose to modify the impregnation method, as this is a relatively noncomplex procedure that can potentially be scaled up, a feature that is not readily feasible for the sol-immobilization method.

Preparation of Supported AuPd Nanoparticles Using a Modified Impregnation Method

In the coimpregnation method, the small nanoparticles comprised mainly Pd and the Au was deposited mainly in the form of large nanoparticles. This suggests that this method does not lead to the effective dispersion of the Au component and on interaction with the support large Au nanostructures are formed that do manage to incorporate some Pd.

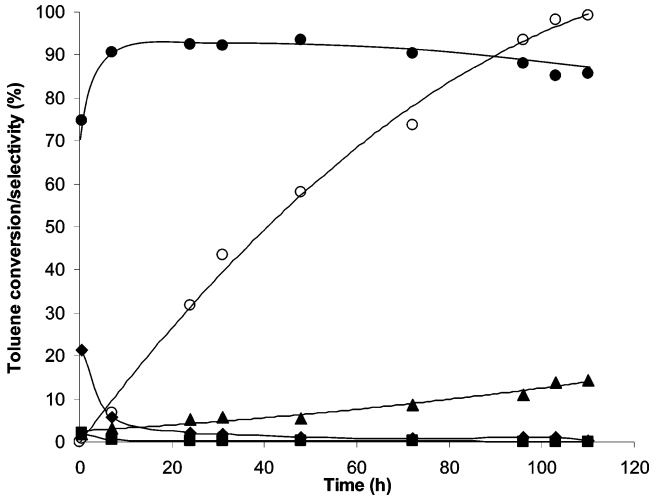

FIGURE 13. Toluene conversion using S_{Im} 1 wt % AuPd/C at 160 °C, 0.1 MPa pO_2, 20 mL of toluene, 0.8 g of catalyst, toluene/metal molar ratio of 3250; (○) conversion, (■) benzyl alcohol selectivity, (◆) benzaldehyde selectivity, (▲) benzoic acid selectivity, and (●) benzyl benzoate selectivity.

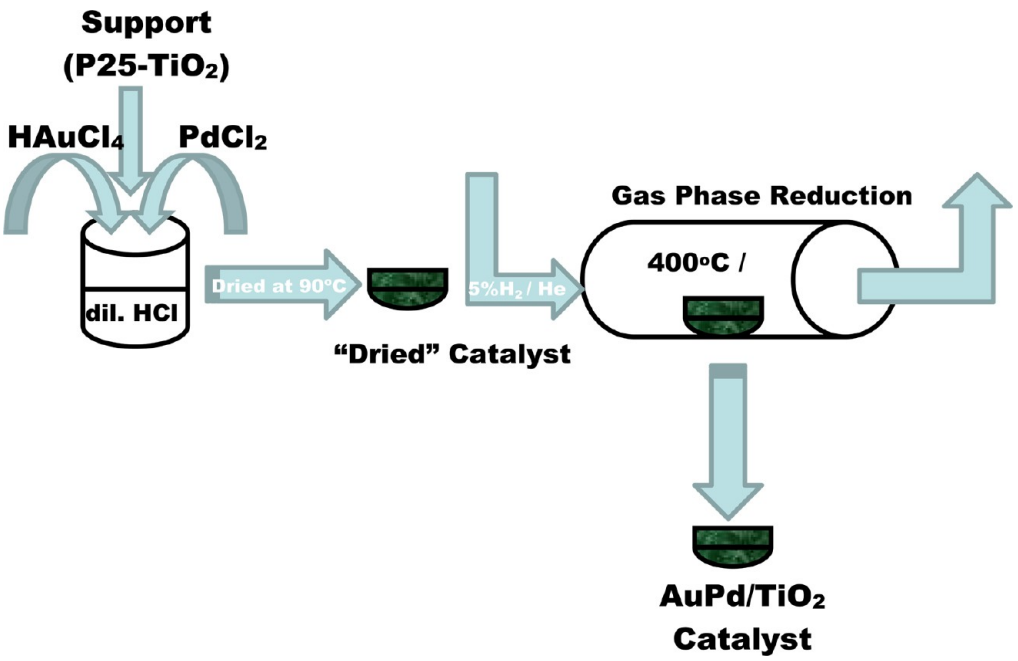

FIGURE 14. M_{Im} preparation method.

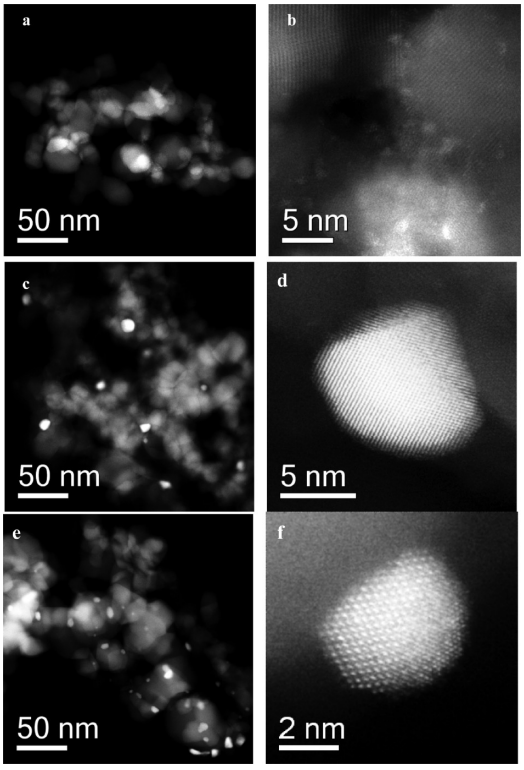

FIGURE 15. HAADF-STEM images of 0.5% Au + 0.5% Pd/TiO_2 catalysts prepared by the C_{Im} method: (a, b) dried only at 120 °C; (c, d) calcined in air at 400 °C; and (e, f) reduced in 5% H_2/Ar at 400 °C.

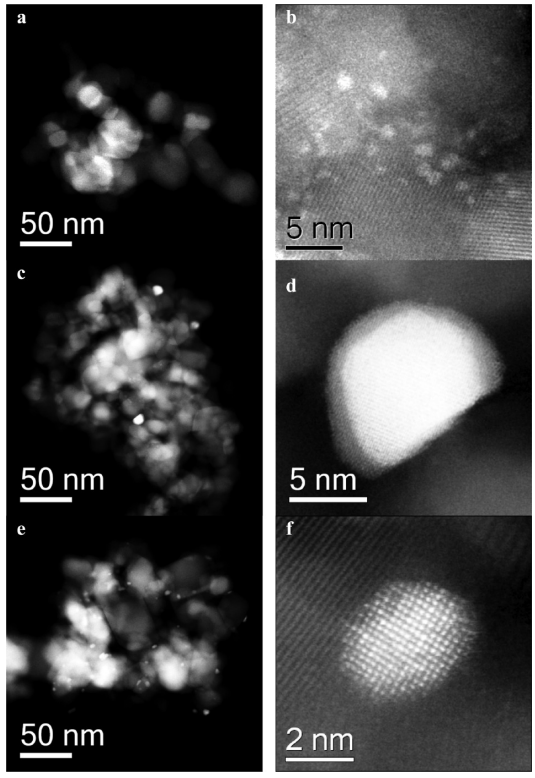

FIGURE 16. HAADF images of 0.5% Au + 0.5% Pd/TiO_2 catalysts prepared by the M_{Im} method with 0.58 M HCl: (a, b) dried only at 120 °C; (c, d) calcined in air at 400 °C; and (e, f) reduced in 5% H_2/Ar at 400 °C.

This is not the case in the sol-immobilsation method where now the gold is highly dispersed and more effectively than the Pd. In order to improve the dispersion of the Au, we have investigated an excess anion method in which we added additional halide to the impregnating solution.[33] In this method, we added aqueous HCl to the water used to

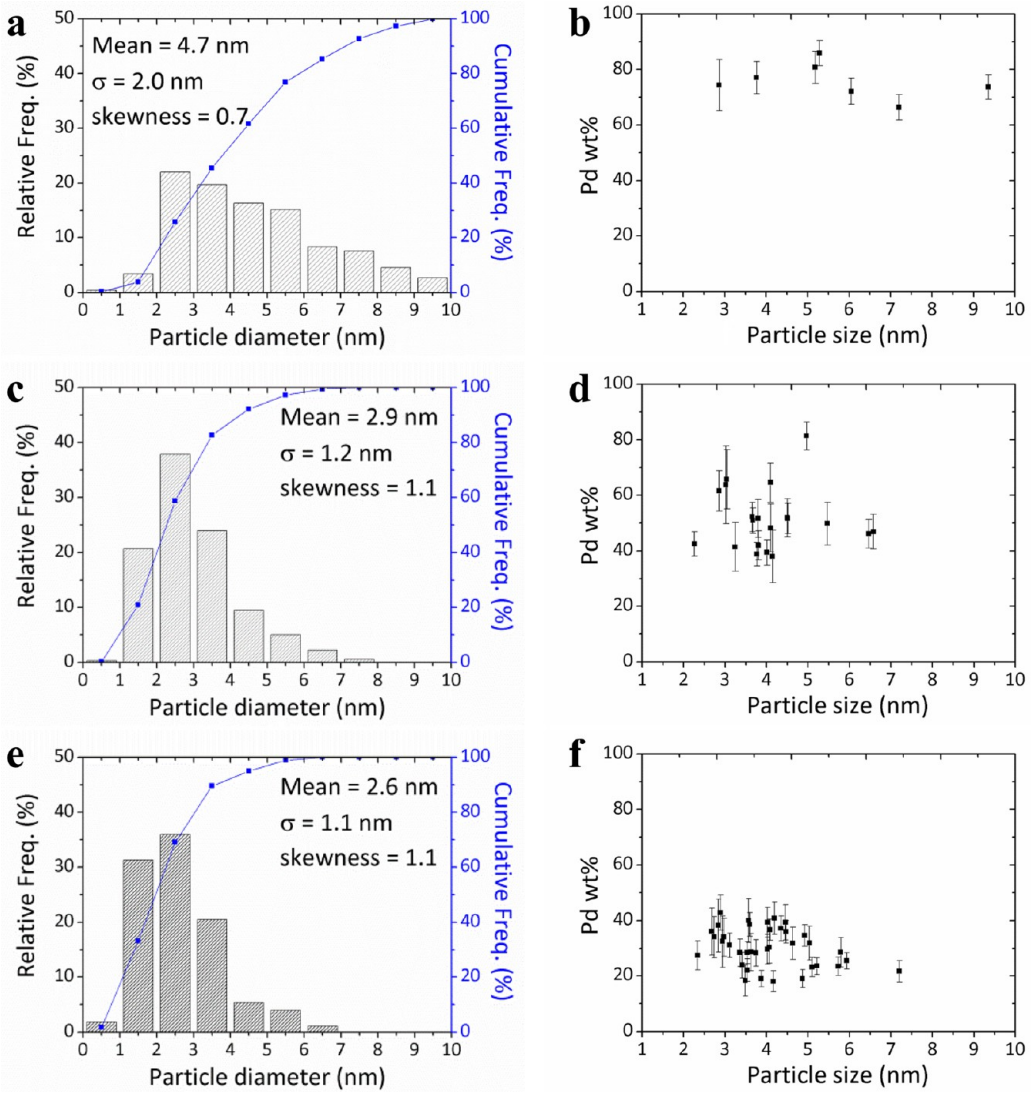

FIGURE 17. Particle size distributions for 0.5% Au + 0.5% Pd/TiO_2 samples prepared with (a) no HCl (i.e., C_{Im}), (c) 0.58 M HCl (M_{Im}), and (e) 2.0 M HCl (M_{Im}). Particle size/composition diagrams for AuPd/TiO_2 samples prepared with (b) no HCl (i.e., C_{Im}), (d) 0.58 M HCl (M_{Im}), and (f) 2.0 M HCl (M_{Im}).

dissolve the $HAuCl_4$ and $PdCl_2$. The solution was used to impregnate TiO_2 and dried as before. However, to remove the halide from the material, we introduced a reduction treatment with H_2 and the whole process is shown schematically in Figure 14. The addition of the excess halide increases the dispersion of the gold, and in its absence we found using SEM that over 95% of the Au was present as large micrometer-sized particles.[33] The larger particles are absent when the excess halide is present. The effect of the excess halide is therefore to aid the dispersion of the gold in the coimpregnation method.

Detailed high angle annular dark field (HAADF) imaging and STEM-XEDS studies were carried out to compare the morphologies of 0.5 wt % Au + 0.5 wt % Pd/TiO_2 catalysts prepared by the C_{Im} and M_{Im} (0.58 M HCl) preparation routes under three distinct conditions, that is, dried-only, calcined at 400 °C, and reduced in 5% H_2/Ar. Representative data for these C_{Im} and M_{Im} samples are shown in Figures 15 and 16, respectively. The dried-only materials show rather similar morphologies. After calcination in air at 400 °C, some sintering occurs and both materials show 5−10 nm particles which have a distinct Au-rich core and Pd-rich shell morphology. In addition, there are still numerous Pd-rich clusters and atomically dispersed species remaining on the TiO_2. Reducing the dried-only materials at 400 °C in 5% H_2/Ar instead of calcination leads to all the clusters and atomically dispersed species being efficiently subsumed into the larger random alloy particles. However, the reduced C_{Im} and M_{Im} materials do show a distinct difference in AuPd particle size distribution, with mean values of 4.7 and 2.9 nm,

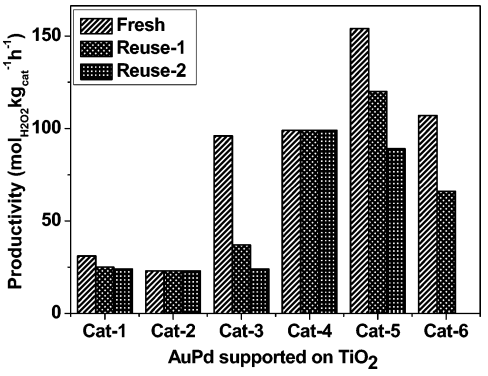

FIGURE 18. Activity and reusability data for H_2O_2 synthesis with 0.5% Au + 0.5% Pd/TiO_2 catalysts prepared by S_{Im} (Cat-1), C_{Im} (Cat-2), and M_{Im} methodologies (Cat-3 through 6), with M_{Im} dried only (Cat-3), reduced in 5% H/Ar at 400 °C/4 h (Cat-4), M_{Im} prepared by NaCl excess (0.58 M) reduced as cat 4 (Cat-5), and M_{Im} prepared by 2 M HCl reduced as cat 4 (Cat-6). Reaction conditions: 5% H_2/CO_2 and 25% O_2/CO_2, 50% H_2/O_2 at 3.7 MPa, MeOH (5.6 g), H_2O (2.9 g), catalyst (0.01 g), 2 °C, 1200 rpm, 30 min.

respectively. So the reduction step in this modified procedure effectively sets up random alloys supported on TiO_2, and the very small nanostructures are now absent.

To determine the effect of the excess halide on the nano structures formed in the catalysts a series of 0.5 wt % Au + 0.5 wt % Pd/TiO_2 catalysts prepared using different Cl concentrations (namely, (i) 0 M HCl (i.e., C_{Im}), (ii) M_{Im} with 0.58 M HCl, and (iii) M_{Im} with 2.0 M HCl) (Figure 17). Following reduction, all the particles are random alloys in nature, but do show a systematic change in Pd/Au ratio with varying Cl concentration. Increasing the amount of excess Cl leads to a definite increase in Au content within the AuPd alloy particles. This is consistent with the gold being more effectively dispersed by the modified impregnation method. However, the key observation is that using the modified impregnation procedure largely eliminates the compositional variation that is observed with the other preparation methods as discussed previously. Hence, by changing the amount of the excess anion, the composition and particle size can be fine-tuned. We have shown that the effects are also observed with other anions, for example, bromide.[33]

Of course, once again, the key question is this: are the new materials prepared by the modified impregnation method effective as catalysts? We have used the direct synthesis of hydrogen peroxide to answer this question.[34] Using a series of catalyst materials with a 1 wt % total metal loading (0.5 wt % Au + 0.5 wt % Pd), we were able to compare the sol-immobilization (S_{Im}) methods with the C_{Im} and M_{Im} routes (Figure 18). It is clear that catalysts prepared by modified impregnation are highly effective and are nearly four times more effective than the AuPd C_{Im} catalyst and S_{Im} catalysts when prepared with the same metal loading, and the catalysts are fully reusable. Interestingly, using NaCl in place of HCl makes an even more active catalyst, but as yet we have not been able to stabilize this for reuse. However, it shows the possibilities for this method. With the M_{Im} method of preparation, it is possible to fine-tune the particle size and control the nanoparticle composition, which was not possible with the standard coimpregnation and sol-immobilization methods.

Concluding Comments

The preparation of supported metal nanoparticles is a topic that attracts significant attention. Much effort is applied to making specific morphologies. In the approaches we have taken, we have at the heart of the experimental protocols focused our attention on making supported nanoparticles that can function as effective catalysts, and they also must be robust and reusable.

We have investigated three experimental strategies for the synthesis of bimetallic nanoparticles, and we stress that the preparation of bimetallic nanoparticles is far more complex than producing their monometallic counterparts. In the case of a single metal, such as gold, the prime concern is control of the particle size distribution; although there are secondary concerns such as the oxidation state on the surface of the metal nanoparticles (which in the case of Au is typically zerovalent) and the interaction between the metal nanoparticles and the support and the specific nanoparticles morphologies that can be formed. However, the addition of a second metal adds significantly to the complexity. Does the addition of the second metal alloy effectively with the first? Do the nanoparticles have a uniform composition? We have demonstrated these complexities using AuPd as an example. It is apparent that the addition of small amounts of Au to Pd and vice versa leads to a significant enhancement in the three reactions we have used as examples in this Account, and these are typical examples of redox reactions that vary in difficulty. The synergistic effect of the combination of the two metals is not considered to originate from a morphological effect but rather an electronic effect, but the precise origin of the effect has yet to be determined.

It is clear that, of the three preparation methods we describe, the coimpregnation method gives the most diverse range of supported nanostructures. Yet it also produces materials that have excellent catalytic activity for alcohol oxidation and hydrogen peroxide synthesis. As we have

noted earlier, from a catalyst design standpoint, this method produces such a range of structures that some should be effective for the chosen catalytic application. For this reason, we typically select C_{Im} as our starting point when designing catalysts for a new reaction. However, with respect to selectivity, this relatively simple method far outperforms other methods of preparation. Hence, for alcohol oxidation and hydrogen peroxide synthesis, it is apparent that larger nanoparticles are the effective catalytic entities. This is in contrast to many experimental approaches where the aim is to produce very small nanoparticles. Coupling the synthesis of supported nanoparticles with their use as catalysts shows that a different range of nanostructures can be preferred. For example, in the more demanding reaction of toluene oxidation, the much smaller nanoparticles made by sol-immobilization are effective, and hence the particle size has to be fine-tuned to the specific catalytic application.

We have emphasized that one key problem when dealing with bimetallic nanoparticles concerns the control of the composition of the individual nanoparticles. With C_{Im} and S_{Im}, we have shown that the interparticle composition varies significantly with particle size. This will have major consequences for any potential application, not just catalysis. However, we have recently shown that adding excess halide in the impregnation methodology, coupled with a reduction step, leads to alloyed nanoparticles that have uniform compositions. Furthermore, the composition in the AuPd system can be controlled by the amount of the excess halide that is used. These materials, when optimized, are very active and reusable catalysts.

There are clearly a wide range of potential experimental strategies for the synthesis of bimetallic nanoparticles. In this Account, we have described and discussed the three approaches we have studied in detail over the past decade. The three methods exemplify the key problems that require attention: namely, how can the particle size distribution and the nanoparticle composition be effectively controlled? We have shown how this can be achieved and that the nanostructures produced are highly effective as catalysts; however, of course, there is still room for much improvement. In addition, we have only focused on the synthesis of the bimetallic nanoparticles, although the interface between the nanoparticles and the support can be very important in defining the catalytic activity that can be expected. In this sense, the synthesis of the support is equally important as in many cases it is an integral part of the catalyst. Hence, designing and fabricating active catalysts requires the optimization of many factors, and we hope that this Account will inspire the design of greatly improved catalysts for the future.

The authors would like a succession of excellent students and postdocs for their invaluable contributions to this work over the past 8 years, especially Drs A. A. Herzing, R. Tiruvalam, and Q. He for their innovative electron microscopy work. and Drs. J. K. Edwards, D. Enache, N. Dimitratos, J. A. Lopez-Sanchez, M. Sankar, and P. Miedziak for excellence in catalyst design.

BIOGRAPHICAL INFORMATION

Graham J. Hutchings, born 1951, studied chemistry at University College London. His early career was with ICI and AECI Ltd where he became interested in gold catalysis. In 1984, he moved to academia and is currently he is Director of the Cardiff Catalysis Institute. He was elected a Fellow of the Royal Society in 2009.

Christopher J. Kiely, born 1962, was educated at Bristol University. Following being a postdoc, he joined Liverpool University, becoming Professor of Materials Chemistry (1999). In 2002, he moved to Lehigh University and is Professor of Materials Science and Chemical Engineering. His research expertise lies in the application and development of electron microscopy techniques for the study of particulate materials.

FOOTNOTES

*To whom correspondence should be addressed. E-mail: hutch@cardiff.ac.uk.
The authors declare no competing financial interest.

REFERENCES

1 Twigg, M. V. *Catalyst Handbook*; Manson, London, UK, 1996.
2 Bond, G. C.; Thompson, D. T. Catalysis by Gold. *Cat. Rev. — Sci. Eng.* **1999**, *41*, 319–388.
3 Hutchings, G. J. Vapor phase hydrochlorination of acetylene: Correlation of catalytic activity of supported metal chloride catalysts. *J. Catal.* **1985**, *96*, 292–295.
4 Nkosi, B.; Coville, N. J.; Hutchings, G. J. Reactivation of a supported gold catalyst for acetylene hydrochlorination. *J. Chem. Soc., Chem. Commun.* **1988**, 71–72.
5 Haruta, M.; Kobayashi, T.; Sano, H.; Yamada, N. Novel gold catalysts for the oxidation of carbon-monoxide at a temperature far below 0 °C. *Chem. Lett.* **1987**, 405–408.
6 Haruta, M.; Yamada, N.; Kobayashi, T.; Iijima, S. Gold catalysts prepared by coprecipitation for low-temperature oxidation of hydrogen and of carbon monoxide. *J. Catal.* **1989**, *115*, 301–309.
7 Haruta, M. Gold as a novel catalyst in the 21st century: Preparation, working mechanism and applications. *Gold Bull.* **2004**, *37*, 27–36.
8 Haruta, M.; Daté, M. Advances in the catalysis of Au nanoparticles. *Appl. Catal., A* **2001**, *222*, 427–437.
9 Hughes, M. D.; Xu, Y.-J.; Jenkins, P.; McMorn, P.; Landon, P.; Enache, D. I.; Carley, A. F.; Attard, G. A.; Hutchings, G. J.; King, F.; Stitt, E. H.; Johnston, P.; Griffin, K.; Kiely, C. J. *Nature* **2005**, *437*, 1132–1135.
10 Carrettin, S.; Concepción, P.; Corma, A.; López Nieto, J. M.; Puntes, V. F. Nanocrystalline CeO_2 increases the activity of Au for CO oxidation by two orders of magnitude. *Angew. Chem., Int. Ed.* **2004**, *43*, 2538–2540.
11 Fu, Q.; Saltsburg, H.; Flytzani-Stephanopoulos, M. Active nonmetallic Au and Pt species on ceria-based water-gas shift catalysts. *Science* **2003**, *301*, 935–938.
12 Corma, A.; Garcia, H. Supported gold nanoparticles as catalysts for organic reactions. *Chem. Soc. Rev.* **2008**, *37*, 2096–2126.
13 Corma, A.; Serna, P. Chemoselective hydrogenation of nitro compounds with supported gold catalysts. *Science* **2006**, *313*, 332–334.
14 Della Pina, C.; Falletta, E.; Prati, L.; Rossi, M. Selective oxidation using gold. *Chem. Soc. Rev.* **2008**, *37*, 2077–2095.
15 Hashmi, A. S. K.; Hutchings, G. J. Gold Catalysis. *Angew. Chem., Int. Ed.* **2006**, *45*, 7896–7936.

16 Haruta, M. Spiers Memorial Lecture, Role of perimeter interfaces in catalysis by gold nanoparticles. *Faraday Discuss.* **2011**, *152*, 11–32.

17 Herzing, A. A.; Kiely, C. J.; Carley, A. F.; Landon, P.; G.J. Hutchings, G. J. Identification of active gold nanoclusters on iron oxide supports for CO oxidation. *Science* **2008**, *321*, 1331–1335.

18 Turner, M.; Golovko, V. B.; Vaughan, O. P.; Abdulkin, P.; Berenguer-Murcia, A.; Tikhov, M. S.; Johnson, B. F. G.; Lambert, R. M. Selective oxidation with dioxygen by gold nanoparticle catalysts derived from 55-atom clusters. *Nature* **2008**, *454*, 981–983.

19 Edwards, J. K.; Hutchings, G. J. Palladium and gold−palladium catalysts for the direct synthesis of hydrogen peroxide. *Angew. Chem., Int. Ed.* **2008**, *47*, 9192–9198.

20 Enache, D. I.; Edwards, J. K.; Landon, P.; Solsona-Espriu, B.; Carley, A. F.; Herzing, A. A.; Watanabe, M.; Kiely, C. J.; Knight, D. W.; Hutchings, G. J. Solvent-free oxidation of primary alcohols to aldehydes using Au-Pd/TiO_2 catalyst. *Science* **2006**, *311*, 362–365.

21 Kesavan, L.; Tiruvalam, R.; Ab Rahim, M. H.; bin Saiman, M. I.; Enache, D. I.; Jenkins, R. L.; Dimitratos, N.; Lopez-Sanchez, J. A.; Taylor, S. H.; Knight, D. W.; Kiely, C. J.; Hutchings, G. J. Solvent-Free Oxidation of Primary Carbon-Hydrogen Bonds in Toluene Using Au-Pd Alloy Nanoparticles. *Science* **2011**, *331*, 195–199.

22 Brett, G.; He, Q.; Hammond, C.; Miedziak, P. J.; Dimitratos, N.; Sankar, M.; Herzing, A. A.; Conte, M.; Lopez-Sanchez, J. A.; Kiely, C. J.; Knight, D. W.; Taylor, S. H.; Hutchings, G. J. Selective Oxidation of Glycerol by Highly Active Bimetallic Catalysts at Ambient Temperature under Base-Free Conditions. *Angew. Chem., Int. Ed.* **2011**, *50*, 10136–10139.

23 Pritchard, J. C.; He, Q.; Ntainjua, E. N.; Piccinini, M.; Edwards, J. K.; Herzing, A. A.; Carley, A. F.; Moulijn, J. A.; Kiely, C. J.; Hutchings, G. J. The effect of catalyst preparation method on the performance of supported Au-Pd catalysts for the direct synthesis of hydrogen peroxide. *Green Chem.* **2010**, *12*, 915–921.

24 Edwards, J. K.; Carley, A. F.; Herzing, A. A.; Kiely, C. J.; Hutchings, G. J. Direct synthesis of hydrogen peroxide from H_2 and O_2 using supported Au-Pd catalysts. *Faraday Discuss.* **2008**, *138*, 225–239.

25 Herzing, A. A.; Watanabe, M.; Edwards, J. K.; Conte, M.; Tang, Z.-R.; Hutchings, G. J.; Kiely, C. J. Energy dispersive X-ray spectroscopy of bimetallic nanoparticles in an aberration corrected scanning transmission electron microscope. *Faraday Discuss.* **2008**, *138*, 337–351.

26 Edwards, J. K.; Solsona, B.; N, E. N.; Carley, A. F.; Herzing, A. A.; Kiely, C. J.; Hutchings, G. J. Switching-off hydrogen peroxide hydrogenation in the direct synthesis process. *Science* **2009**, *323*, 1037–1041.

27 Edwards, J. K.; Pritchard, J.; Piccinini, M .; Shaw, G.; He, Q.; Carley, A. F.; Kiely, C. J.; Hutchings, G. J. The effect of heat treatment on the performance and structure of carbon-supported Au-Pd catalysts for the direct synthesis of hydrogen peroxide. *J. Catal.* **2012**, *292*, 227–238.

28 Comotti, M.; Della Pina, C.; Matarrese, R.; Rossi, M. The Catalytic Activity of "Naked" Gold Particles. *Angew. Chem., Int. Ed.* **2004**, *43*, 5812–5815.

29 Tiruvalam, R. C.; Pritchard, J. C.; Dimitratos, N.; Lopez-Sanchez, J. A.; Edwards, J. K.; Carley, A. F.; Hutchings, G. J.; Kiely, C. J. Aberration corrected analytical electron microscopy studies of sol-immobilized Au + Pd, Au{Pd} and Pd{Au} catalysts used for benzyl alcohol oxidation and hydrogen peroxide productio. *Faraday Discuss.* **2011**, *152*, 63–86.

30 Pritchard, J.; Kesavan, L.; Piccinini, M.; He, Q.; Tiruvalam, R.; Dimitratos, N.; Lopez-Sanchez, J. A.; Carley, A. F.; Edwards, J. K.; Kiely, C. J.; Hutchings, G. J. Direct synthesis of hydrogen peroxide and benzyl alcohol oxidation using Au-Pd catalysts prepared by sol immobilization. *Langmuir* **2010**, *26*, 16568–16577.

31 Comotti, M.; Li, W.-C.; Spliethoff, B.; Schüth, F. Support effect in high activity gold catalysts for CO oxidation. *J. Am. Chem. Soc.* **2006**, *128*, 917–924.

32 Lopez-Sanchez, J. A.; Dimitratos, N.; Hammond, C.; Brett, G. L.; Kesavan, L.; White, S.; Miedziak, P.; Tiruvalam, R.; Jenkins, R. L.; Carley, A. F.; Knight, D. W.; Kiely, C. J.; Hutchings, G. J. Facile removal of stabilizer-ligands from supported gold nanoparticles. *Nat. Chem.* **2011**, *3*, 551–556.

33 Sankar, M.; He, Q.; Morad, M.; Pritchard, J.; Freakley, S. J.; Edwards, J. K.; Taylor, S. H.; Morgan, D. J.; Carley, A. F.; Knight, D. W.; Kiely, C. J.; Hutchings, G. J. Synthesis of stable ligand-free gold-palladium nanoparticles using a simple excess anion method. *ACS Nano* **2012**, *6*, 6600–6613.

34 Edwards, J. K.; Solsona, B. E.; Landon, P.; Carley, A. F.; Herzing, A.; Kiely, C. J.; Hutchings, G. J. Direct synthesis of hydrogen peroxide from H_2 and O_2 using TiO_2-supported Au−Pd catalysts. *J. Catal.* **2005**, *236*, 69–79.